



SRTTU

Journal of Computational and Applied Research
in Mechanical Engineering

jcarme.sru.ac.ir

JCARME

ISSN: 2228-7922

Research paper

Effect of exhaust gas recirculation and constant pre-heated air temperature on the homogeneous charge compression ignition combustion engine with diesel and WPPO 20 blend

R. Jyothu Naik^{a,*}, K. Thirupathi Reddy^b and S. Vishal Narayanrao^c

^aMechanical Engineering, Rayalaseema University College of Engineering Kurnool, Andhra Pradesh, 518007, India

^bMechanical Engineering RGM CET, Nandyal, Andhra Pradesh, 518501, India

^cMechanical Engineering, Sandip University, Mahiravani, Trimbak Road, Nashik (MS), 422 213, India

Article info:

Article history:

Received: 16/09/2021

Accepted: 18/12/2023

Revised: 21/12/2023

Online: 23/12/2023

Keywords:

Preheated air temperature,

Exhaust gas recirculation,

Port fuel injection,

Waste plastic pyrolysis oil,

Emissions.

*Corresponding author:

jyothu.naik@gmail.com

Abstract

This article describes an experimental study on fueling the port fuel injection homogeneous charge compression ignition (PFI-HCCI) combustion engine with plastic oil that is generated from waste plastics through the pyrolysis method. The study tested different exhaust gas recirculation (EGR) levels of 0%, 5%, 10%, and 15% using a modified PFI-HCCI computerized 4-stroke, single-cylinder, water-cooled, direct injection Kirloskar diesel engine connected to an eddy current dynamometer. Furthermore, an engine running at 1500 rpm and a constant preheated air temperature (PHAT) of 140°C were assessed. In this experiment, fuel, 20% biodiesel waste plastic pyrolysis oil (WPPO), and continuous PHAT 140°C are used. The testing results show that the cylinder peak pressure and heat release rate for WPPO 20 with 15% EGR were attained at 39.70% and 15.09%, respectively. Additionally, port fuel injection with PHAT and WPPO 20% without EGR is reported to have a 45% higher brake thermal efficiency at full load in comparison to PFI-HCCI Diesel (D100). But when employed at full load with 15% EGR, the WPPO 20 blend also reduced smoke opacity by 30.74% and Oxides of Nitrogen (NO_x) emission by 52.17%. On the other hand, compared to the PFI-HCCI (D100), there are higher emissions of carbon monoxide (CO) (22.07%) and unburnt hydrocarbon (UHC) (54.14%) with 15% EGR. Consequently, WPPO can be used for the PFI-HCCI engine.

1. Introduction

Novel combustion techniques were examined to instantly decrease NO_x and the soot releases in predictable diesel engines in light of increasingly

strict emission regulations. An advantageous alternative combustion technique with reduced emissions of soot and NO_x and increased efficiency is homogeneous charge compression ignition (HCCI). Numerous researchers

studying HCCI combustion suggested that NO_x and particular matter (PM) emissions might be reduced [1]. However, before it can be used in automobiles for commercial purposes, a number of issues need to be fixed. The PFI-HCCI combustion engine presents greater (UHC) and CO emissions and is generally difficult to control the timing of combustion [2]. The port fuel injection method, which requires installing the injector in the intake manifold near the intake valve, is the simplest approach to creating the outside mixture. This method improves fuel distribution and volumetric efficiency through carburetion. To evaporate petrol in the intake manifold, a few researchers have experimented raising the temperature of the intake air. A biodiesel blend made from waste plastic pyrolysis oil, variable inlet air temperature, and external port fuel injection were used in experiments on an HCCI engine. Blends of WPPO biodiesel were used in the experiment. Four blending ratios (volume basis) of diesel (D) were employed in an HCCI engine: WPPO5, WPPO10, WPPO15, and WPPO20. At varying loads, the intake charge's temperature ranges were adjusted to 80°C, 100°C, 120°C, and 140°C. Raising the intake charge temperature led to a slight increase in CO and UHC emissions but a significant increase in brake thermal efficiency. Despite somewhat increased UHC and CO emissions, the results showed that the brake thermal efficiency was 45.12 percent at 140°C and WPPO20, the input air temperature and WPPO20 [3]. Using an external PFI, vaporizer technology, and a waste plastic pyrolysis oil biodiesel blend, some experiments were conducted on an HCCI engine. The author concluded that at a WPPO 20% biodiesel blend, better brake thermal efficiency (BTE) was found at 37% without exhaust gas recirculation (EGR). The results of another study [4]. indicate that the best method for regulating the rate of combustion and NO_x production is to use EGR. To prevent early ignition in HCCI tests, the port fuel injection system was used in conjunction with a cooled EGR and a fuel vaporizer. The results showed that minor emissions of NO_x and smoke were produced at an EGR rate of 30% [5]. The researchers created an atomizer for mixture preparation and examined how engine speed, intake air temperature, and EGR affected HCCI

combustion. Based on the findings, the authors concluded that EGR is a useful technique for lowering NO_x and combustion rate [6]. WPPO biodiesel blends diesel (D) in an HCCI-direct injection engine was blended at four different ratios (volume basis) to compare the engine's performance, emissions, and combustion characteristics to neat diesel while accounting for engine gas injection (EGR). According to the examination, HCCI-direct injection combustion produced somewhat more NO_x at delayed start of pilot injection (SoPI) timing 30° before top dead center (bTDC), but innovative SoPI timings (40° bTDC), HCCI-direct injection combustion was observed to result in comparatively lower engine performance [7]. The creation of a technique that allows for the achievement of a totally homogenous fuel-air mixture was necessary for the current experimental study. To convert an engine to an HCCI engine, a few minor equipment modifications are needed. For the aforementioned rationale, this study uses an air heater to investigate the basic properties of HCCI combustion. With an air heater, a homogenous mixture of fuel droplets and air forms due to excellent mixing in the vaporizer. The studies included a range of diesel and WPPO 20% biodiesel mixtures, as well as various engine loads (25, 50, 75, and 100%) and EGR levels (5%, 10%, and 15%). The cylinder pressure, the HCCI's smoke emission, the Rate of Heat Release (RoHR), BTE, exhaust gas temperature (EGT), NO_x, CO, and UHC were also observed.

2. Material and experimental methodology

2.1. Waste plastic pyrolysis oil biodiesel preparation

Plastic rubber production has expanded dramatically in the global market since 1975, owing to the rising use of plastics [8]. It should come as no surprise that 15000 tonnes of plastic garbage are created daily, of which 9000 tonnes are collected and prepared, given that plastic waste is a significant source of municipal solid waste. Nevertheless, 6000 tonnes of trash plastic are not gathered causing real natural problems as they enter the organic systems of sensitive

marine life. Plastic waste is abundant, and some of the costs associated with collecting, sorting, and washing it are avoided [9]. It has water bottles, bags, etc., which have been dropped as solid waste in the natural environment.

The waste plastics pyrolysis machine setup is depicted in Fig. 1. It has water packets that were ruined when mineral water was put inside them. There is no need to wash it because it does not contain any dust particles, although it might contain dampness. There is a possibility that the packets will release carbon dioxide if there is any moisture present. To rid the packets of moisture, we must dry them. The polymers can be fed into the reactor once the cutting and drying processes are finished. Weighing the input plastics before feeding them into the reactor will allow us to determine the potential fuel yield. Here, the catalyst is barium carbonate powder. This catalyst lowers the cracking temperature and improves the fuel's purity at the same time. The plastic first becomes liquid when heated, and intense heating eventually causes the polymer chain to break, vaporizing the material. During this procedure, plastics are heated between 300 and 450°C at air pressure. Only the plastics then experience several oligomer cracks, leading to monomer combinations in the end.



Fig. 1. Waste plastics collected.



Fig. 2. Pyrolysis equipment.

Our review of the literature indicates that even though a catalyst lowers the temperature at which cracking occurs, we still need continuing the same temperature range as thermal cracking to convert plastics into oil more effectively. In a 10:1 ratio, we introduce catalysts to the plastics [10]. According to our survey, introducing catalysts in various ratios had no discernible effect on the process. Since our plastic weighs 1.5 kg, we have added 150 gr of powdered barium carbonate. Here, we employ a band-style heater to heat the reactor from the outside in. We were able to maintain the necessary temperature within reactor by employing temperature controller and contactor arrangement. Around 270°C is when plastic begins to fracture, and between 370 and 390°C is when we may obtain the best amount of the cracked monomer mixture. These high-temperature vapors enter the condenser to cool after passing through the pipes [9]. The condenser receives the vapors that are released from inside the reactor via pipes. Water comes into touch with the copper spiral tube that makes up the condenser pipe. The water inside the chamber senses the heat that vapours that enters the condenser pipe exchange with the copper pipes as they cool. As a result, vapors are cooled into liquids that are at normal temperatures. These liquids are gathered from the condenser's outflow pipe. This liquid is nothing more than the pyrolyzed waste plastic oil we used. The pyrolysis apparatus is depicted in Fig. 2.

3. Material and fuel properties

3.1. Fuel properties

Diesel fuel and waste plastic pyrolysis oil were employed in this study. First came the creation of WPPO, which was obtained by burning waste plastic. In the second stage, diesel fuel and waste plastic pyrolysis oil biodiesel were combined at a volume-based ratio of 20% and 20%, respectively, to form WPPO 20. Regarding the features of the engine and the combustion process, viscosity is the most crucial factor [11-12]. As a result, blend density (ρ) was calculated using Eq. (1), and blend viscosity (ν) at 40°C was estimated using Eq. (2), the cetane number of combinations was assessed using Eq. (3), and the heat value of the mixed fuel was estimated using Eq. (4).

$$\rho_b = \sum_{i=1}^3 X_i \rho_i \quad (1)$$

$$\ln v_b = \sum_{i=1}^3 X_i \ln v_i \quad (2)$$

$$C_{n,b} = \sum_{i=1}^3 X_i C_{n,i} \quad (3)$$

$$H_{v,b} = \frac{\sum_{i=1}^3 X_i \rho_i H_{v,i}}{\sum_{i=1}^3 X_i \rho_i} \quad (4)$$

3.2. Experimental methodology

The research engine was a four-stroke, single-cylinder, direct injection, computerised, and water-cooled engine. Apex Innovation Ltd., located in Sangli, supplied a diesel engine of the Kirloskar Tv1 type for research purposes. To operate in the Hcci mode, this engine has been changed. It was decided to use port fuel injection systems with PHATs as an external technique for mixture generation. Fig. 3, shows the schematic diagram of the experimental setup. Apex Innovations Pvt. Ltd. developed an engine soft, a lab view-based software programme for monitoring engine performance. Most engine testing application requirements, such as data entry, reporting, monitoring, and logging, may be handled by Engine Soft. The program assesses combustion parameters, fuel economy, and engine efficiency. Different graphs are produced by different operation modes. Online engine testing in run condition reads, stores, and displays critical signals in the graph. You can view the data in tabular, graphical, and data formats by opening the stored data file. The data in Excel format can be utilized for the upcoming study. A photographic perspective is displayed in Fig. 3 and Fig. 4, which show a schematic design of the experimental setup. Fig. 5 shows the BOSCH gas petrol solenoid injector and air heater is shown in Fig. 6. Tables 1 and 2 show the engine specifications as well as the properties of waste plastic pyrolysis oil and diesel. An electronic control unit (ECU) controlled the PFI. Fig. 7, shows the photographic perspective of the system. Fuel quantity and timing are managed by the ECU. Without growing the backpressure in the exhaust pipe, the exhaust gases were taken to an inspecting line to estimate emissions.

Fig. 8 displays the Airrex 5-gas emission analyzer, whereas Fig. 9 displays the traditional smoke metre.

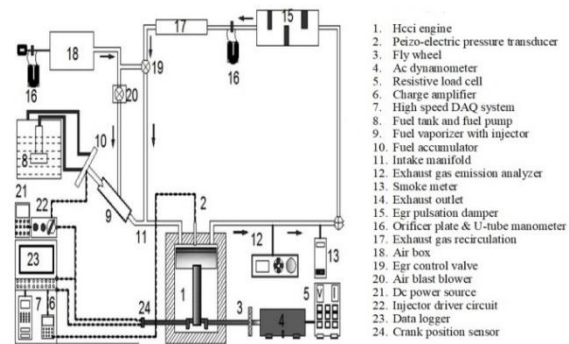


Fig. 3. Schematic diagram of the experimental setup.



Fig. 4. Photographical view of the experimental setup.



Fig. 5. Port fuel injector.



Fig. 6. Air heater.



Fig. 7. Photo graphical view of ECU.

Table 1. Experimental engine specifications.

S. no	Parameter	Description
1	Make	Kirloskar
2	Model	Tv1
3	Bore x stroke	87.5 mm × 110 mm
4	Swept volume	661.45 cc
5	Connecting rod	234.00 mm
6	Compression ratio	18:1
7	Rate speed	1500 rpm

Table 2. Properties of diesel, waste plastic pyrolysis oil.

S. no	Propertie	Diesel	Waste plastic pyrolysis oil
1	Colour	Orange	Black
2	Specific gravity at 30°C	0.88	0.822
3	Kinematic viscosity at 40°C (cSt)	3.0	2.3
4	Calorific value (kJ/kg)	46300	42100
5	Flash point (30°C)	>51	37
6	Fire point (30°C)	>55	40
7	Cetane number	55	52



Fig. 8. Photo graphical view of avl 437 standard smoke meter.

It is employed to gauge engine emissions. Here are the typical results, which were all consistently estimated for three minutes. To ensure that the results are repeatable within the experimental uncertainties, each test was conducted twice.

Uncertainty of error

$$\begin{aligned}
 &= \sqrt{((\text{speed sensor})^2 + (\text{pressure transducer})^2 + (\text{crank angle encoder})^2 + (\text{charge amplifier})^2} \\
 &\quad \sqrt{+(\text{load indicator})^2 + (\text{egt indicator})^2 + (\text{NO}_x)^2 + (\text{CO})^2 + (\text{Uhc})^2 + (\text{Smoke meter})^2)} \\
 & \hspace{15em} (5) \\
 &= \sqrt{((1)^2 + (0,2)^2 + (0,01)^2 + (0,1)^2 + (0,2)^2 + (0,14)^2 + (0,5)^2 + (1)^2 + (1)^2 + (1)^2)} \\
 &= \pm 2.08.
 \end{aligned}$$



Fig. 9. Photo graphical view of airreX5-gas emission analyzer.”

3.3. Uncertainty

To improve the precision of the findings, an experimental process uncertainty assessment must be conducted. Four analyses are conducted to improve the accuracy of the results. An approximation resulting from the equipment used in the experiment is an experiment mistake. Using the relationship given in Eqs. (5), [13,14], the uncertainty analysis was performed based on the parameters [15], such as accuracy, range, and uncertainties of the instruments. It was discovered that the average uncertainty of the experiments was ± 2.08, a level appropriate for experimental activities. The uncertainties of the experiments are presented in Table 3.

Table 3. Uncertainties in the experiment.

Instrument used	Range	Accuracy	Uncertainty (%)
Gas analyser	NO _x 0-5200 ppm	±40 ppm ±0.5	±0.5
	CO 0-10%	±0.03%	±1
	Uhc 0-3000 ppm	±10 ppm	±1
Smoke meter	0-100%	±0.9	±1
Egt indicator	0-800°C	±1°C	±0.14
Pressure transducer	0-110 bar	±0.2	±0.2
Speed sensor	0-10000 rpm	±10 rpm	±1
Crank angle encoder	0-720°CA	±0.4°	±0.01
Charge amplifier		±1	±0.1
Load indicator	250-5500 w	±10	±0.2

3.4. Heat release rate

Based on the collected data, the heat release rate is analyzed using the zero-dimensional heat release model [16]. Eq. (6), was utilized to calculate HRR.

$$\frac{dQ}{d\theta} = \frac{\gamma}{\gamma-1} P \frac{dV}{d\theta} + \frac{1}{\gamma-1} V \frac{dP}{d\theta} \quad (6)$$

where pressure, volume, ratio of specific heats, crank angle, and heat release are represented by the letters Q, θ , γ , P, and V, respectively. There are definitions for $dV/d\theta$ and $dP/d\theta$ investigative pressure traces given [17].

The ratio of certain temperatures used in the previously mentioned equation was found using Eq. (7).

$$\gamma = \gamma_o - \frac{k}{100} \frac{T}{1000} \quad (7)$$

γ_o represents the γ value at a base temperature which is typically 300 K. γ_o is determined by the gas composition. γ is usually 1.4 for ambient air and 1.38 for lean air-fuel mixtures. The constant k is typically fixed at 8. The same k value is used for readings on both HCCI-DI and conventional diesel engines [18, 19].

4. Results and discussion

4.1. Cylinder pressure

In Fig. 10, the variation of cylinder pressure for crank angle is illustrated by comparing PFI-HCCI operation of a waste plastic pyrolysis oil (WPPO) biodiesel blend to the PFI-HCCI diesel operation. The tested fuels' cylinder peak pressures are 45 bar and 53 bar, respectively, for WPPO 20 running at full load with 15% EGR and HCCI operating at full load with 15% EGR. The graph shows that for Waste Plastic Pyrolysis Oil (WPPO), the cylinder peak pressure is 15.09 percent higher than for diesel PFI-HCCI operation. Because the biodiesel produced from waste plastics pyrolysis oil has a higher peak pressure, there is a longer delay in inflammation WPPO. The high cylinder pressure was associated with a larger binding ratio because the amount of fuel injected rose as the number of combustions increased, leading to a bigger maximum cylinder pressure. With HCCI, combustion occurs within the cylinder and at a very high combustion rate. Temperature and

drug concentration affect how intensely a material burns. An approach that is more representative and similar to HCCI is the heat release analysis. The simultaneous induction of homogeneous mixing by compression distinguishes the HCCI heat release pattern from that of conventional engines [20].

4.2. Heat release rate

For both the diesel PFI-HCCI operation and the WPPO 20 biodiesel mix PFI-HCCI operation, Fig. 11. shows a comparison of the Heat Release rate change with the crank angle. The heat release rate values for the tested fuels of PFI-HCCI operating at these levels are 41 J/CAD for PFI-HCCI running at a full load of diesel at 15% EGR and 68 J/CAD for WPPO 20 at 15% EGR. The Heat Release Rate for Waste Plastic Pyrolysis Oil (WPPO) is 39.70% higher than the diesel PFI-HCCI operation, as the diagram shows. Heat output during the pre-combustion phase causes longer ignition delays [21].

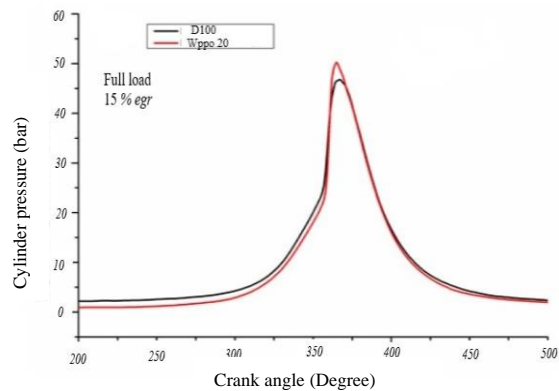


Fig. 10. Variation of cylinder pressure with crank angle.

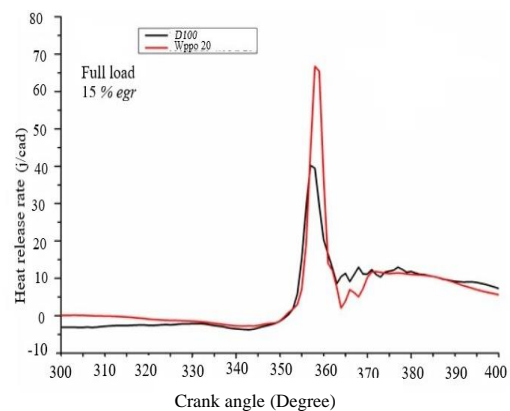


Fig. 11. Variation of rate heat release with crank angle.

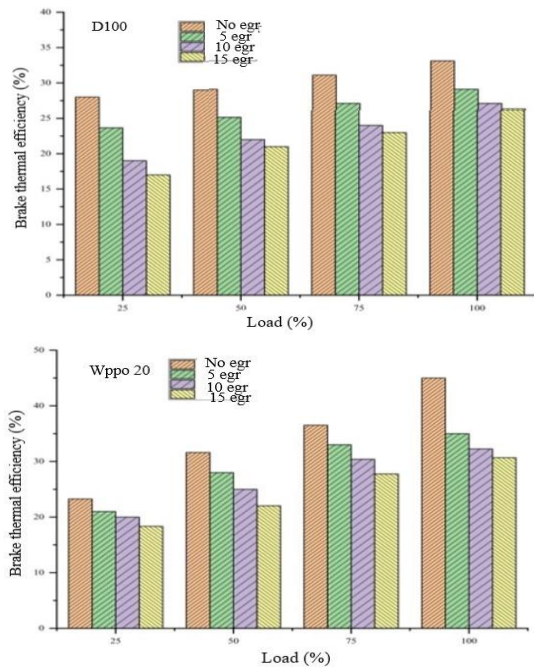


Fig. 12. BTE of diesel and WPPO biodiesel combustion at different load and EGR conditions.

An improvement in EGT is indicated by the higher rate of heat release. The heat release curves for the control fuels show that the two-stage ignition decreases as the amount of biodiesel in the test fuels increases. During the construction of the SoC, it is the computation of non-evaporated fuel droplets. The longer boiling distance of biodiesel leads to a lower rate of dissipation.

4.3. Brake thermal efficiency (%)

The change in BTE with respect to the constant PHAT 140°C is shown in Fig. 12. Along with a comparison between the Diesel PFI-HCCI operation and the WPPO20 biodiesel blend PFI-HCCI mode at varying engine loads and EGR percentages. The chart shows that when the EGR percentage is changed from 0 to 15%, the BTE for a 20% WPPO engine drops from 45% to 30.67% at full load, while for a diesel PFI-HCCI engine, it drops from 33% to 26.22%. It should be noted that in the authors' previous study [22]. The figure shows that lower BTE for lower engine loads at each pre-heated air temperature is caused by the delayed start of combustion. Because of the following factors, HCCI engines should have reduced heat losses: i. a lower combustion temperature; ii. a shorter combustion period; and iii. less soot generation due to the mixture's homogeneous preparation.

Lower HRR and lower combustion temperatures are the outcomes of late burning. The cylinders' absence of heat from the piston and walls improves the piston's performance.

4.4. Exhaust gas temperature

The difference of EGT with the constant PHAT 140°C, with different EGR percentages and various engine loads for the 20% WPPO biodiesel blend PFI-HCCI mode and comparison with the Diesel PFI-HCCI operation is shown in Fig. 13.

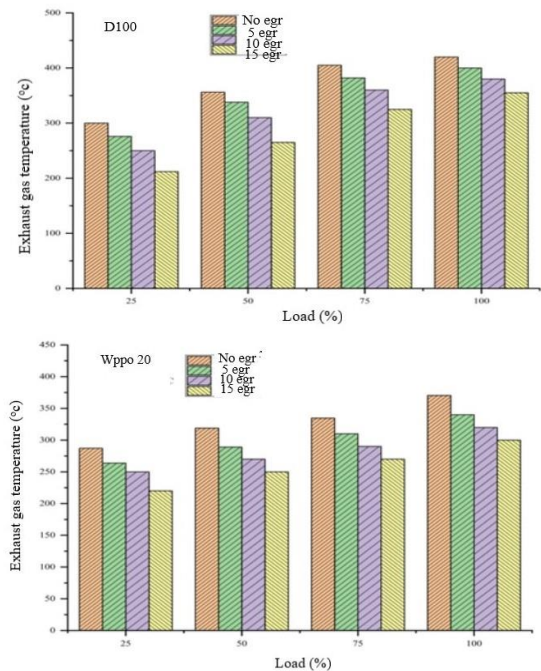


Fig. 13. EGT of diesel and WPPO biodiesel combustion at various load and EGR conditions."

From the figure, it is found that at full load the EGT without EGR is 370.46° C for 20% WPPO and 420°C for diesel fuel. With 15% EGR the EGT is 300°C for 20% WPPO and 355°C for diesel fuel. As the preheated air temperature increases, the start of combustion is accelerated owing to quicker chemical kinetics and reaction rates. Early beginning combustion with a short combustion time increases convective heat transfer as a result of the longer time of residence of the container burning hot gasses. This raises the exhaust gas temperature. One potential reason for low EGT at higher intake air temperature may be prevailing pre-premixed combustion.

4.5. No_x emission

Fig. 14 displays the variation in No_x emissions for the WPPO20 biodiesel blends PFI-HCCI mode and compares it to the Diesel PFI-HCCI operation at constant PHAT 140°C with varying EGR percentages and engine loads. At full load, No_x emissions without EGR and with 5, 10, and 15% EGR from 552 to 340 PPM for 20% WPPO and 700 to 500 PPM for diesel fuel are shown. In terms of (i) the oxidation and nitrogen supply, (ii) burnt gas levels, and (iii) the residence time are three major variables affecting the output of nitric oxide (NO) in a heat engine during the post-flame combustion process. In the combustion chamber's 0068igh-temperature zone, the NO is created. An enlarged Zeldovic method is used to shape each combustor, resulting in no emissions of air nitrogen. Temperature and oxygen concentration mentioned in the preceding equation do not notably affect any formation. The generation of nitric oxide must be prevented by lowering the combustion temperature, as oxygen concentration plays a crucial role in combustion efficiency.

4.6. Carbon monoxide

Fig. 15 describes the variation in CO emission for the 20% WPPO biodiesel blends PFI-HCCI mode at constant PHAT 140° C, with varying EGR percentages and engine loads, and compares it with the Diesel PFI-HCCI operation. According to the figure, there is a corresponding rise in CO emissions of 5%, 10%, and 15% EGR. For 20% WPPO and 0.355 % diesel fuel, the CO Emission at full load without CO emission is 0.1%.

Diesel fuel has a CO emission of 0.405% and 20% WPPO has a CO emission of 0.15% with 15% EGR. As the engine load rises, the CO emission falls. This is a result of rising fuel requirements for high load operations and average cylinder temperature-induced engine load aversion. Either a deficiency of oxygen or oxidation is the cause of CO-release. Lean air/fuel mixes are used in HCCI engines to encourage the full oxidation of the fuel.

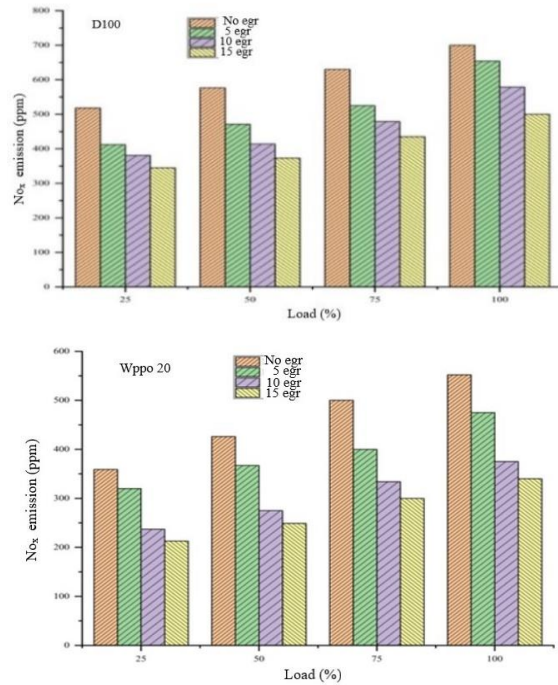


Fig. 14. Diesel and WPPO biodiesel combustion at different load and EGR percentages produce No_x emissions.

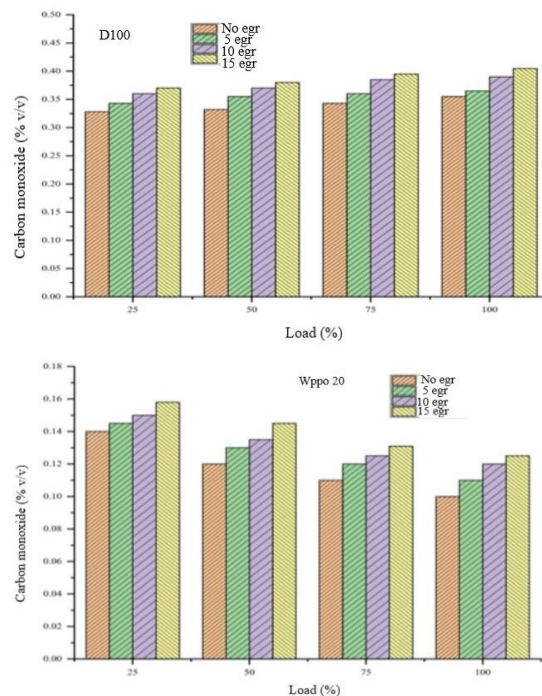


Fig. 15. CO emissions of WPPO oil and diesel at different load and EGR percentages biodiesel combustion.

4.7. Unburned hydrocarbons

The difference in UHC emissions for the 20% WPPO biodiesel blends PFI-HCCI mode and comparison with the Diesel PFI-HCCI operation are shown in Fig. 16. At constant PHAT 140°C with different EGR percentages and engine loads. The figure clearly shows that a 5%, 10%, and 15% increase in EGR is correlated with an increase in UHC emissions. Without an EGR, the UHC emission at full load for 20% WPPO fuel is 65 PPM, and for diesel fuel, it is 43 PPM. The UHC emission with 15% EGR is 82 PPM for diesel fuel and 90 PPM for 20% WPPO. Because of low combustion temperatures, hydrocarbon fuel is burned in HCCI engines, as evidenced by the history of UHC emissions. The combustion temperature is substantially lower close to combustion chamber walls due to the heat losses. The greater portions of UHC pollutants come from the wall areas of the combustion chamber.

4.8. Smoke emission

Fig. 17 shows the variation in smoke opacity for the 20% WPPO biodiesel blends PFI-HCCI mode at constant PHAT 140°C with varying engine loads and EGR percentages and compares it with Diesel PFI-HCCI operation. The figure indicates that as the EGR percentages increase, so does the smoke opacity. Without an EGR, the smoke opacity emission at full load for 20% WPPO and 11% for diesel fuel is 0.1%. The smoke opacity with 15% EGR is 27.9% for 20% WPPO and 20% for diesel fuel. It is necessary to prepare the homogeneous charge for the longer extended ignition delay. The amount of load on the engine and the temperature of the preheated air both reduce smoke emissions. The rise in residence time and oxidation temperature of burning WPPO gases causes smoke emissions to approach nil at 140°C. At 140°C, the lowest recorded smoke emission value for a full load WPPO 20 PFI-HCCI activity is approximately 0.01 percent. The study's total smoke emissions are less than 11%.

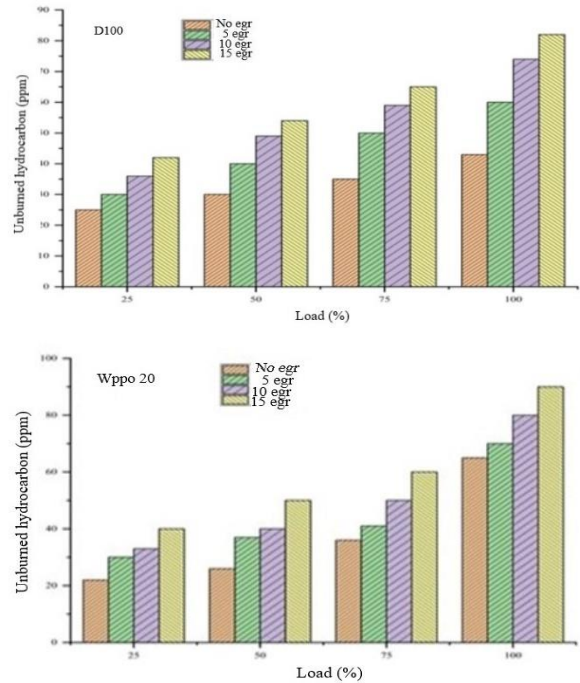


Fig. 16. UHC emissions from burning biodiesel as well as WPPO with different load and EGR percentages.

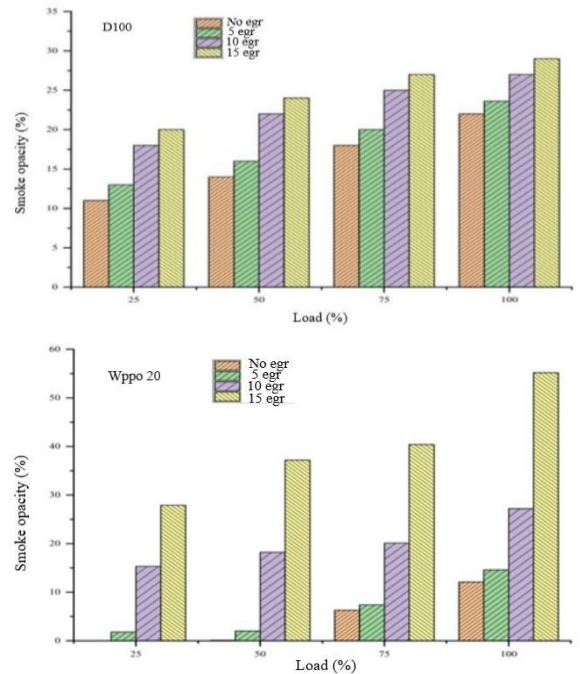


Fig. 17. The amount of smoke produced during the burning of biodiesel and WPPO under varying EGR and load conditions.

5. Conclusions

A two-stage exothermic was observed for HCCI. Low-temperature combustion chemistry drives the first stage of combustion, while high-temperature combustion controls the second stage. The chemical kinetics of WPPO bio-diesel HCCI were reported to be more rapid than those of diesel HCCI. After investigating its impact, it was determined that the optimal method for controlling the HCCI engine is EGR. Without EGR, a higher brake thermal efficiency of 45% was seen with a 20% biodiesel blend in WPPO. By utilizing WPPO 20% with 15% EGR, NO_x emissions are found to be significantly reduced, down to 52.17%. The greatest increase in emissions of CO (22.07%) and UHC (54.14%) was noted in WPPO 20% biodiesel with 15% EGR and a reduction in smoke opacity of up to 30.74% when WPPO 20% is used. HCCI is constrained by the operational framework. The higher load limits combustion noise, whereas the lower load limits CO and UHC emissions. While compared to a traditional engine, the low-temperature combustion approach known as HCCI while using biodiesel has advantages in terms of combustion and engine performance.

References

- [1] B. Harisankar and S. Murugan, "Homogeneous charge compression ignition (HCCI) combustion Mixture preparation and control strategies in diesel engines", *Renew. Sustain. Energy Rev.*, Vol. 38, No. 1, pp. 732-746, (2014).
- [2] R. Jyothu Naik, and K. Thirupathi Reddy, "A review on diesel homogeneous charge compression ignition engine", *Acad. J. Sci Res.*, Vol. 6, No. 8, pp. 321-328, (2018).
- [3] R. Jyothu Naik, and K. Thirupathi Reddy, "Experimental Study on the Effect of Inlet Air Temperature on Waste Plastic Pyrolysis Oil with Diesel Fuelled HCCI Combustion Engine", *Int. J. Recent Technol.*, Vol. 7, No. 1, pp. 158-164, (2019).
- [4] R. Jyothu Naik, and K. Thirupathi Reddy, "Combustion performance and emission characteristics on HCCI engine of waste plastic pyrolysis oil biodiesel blends with external PFI and vaporiser", *Int. J. Sustain Eng.*, Vol. 13, No. 3, pp. 204-217, (2020).
- [5] D. Ganesh, G. Nagarajan, and S. Ganesan, "Experimental investigation of homogeneous charge compression ignition combustion of biodiesel fuel with external mixture formation in a CI engine", *Environ. Sci Technol.*, Vol. 48, No. 5, pp. 3039-3046, (2014).
- [6] S. Midlam-Mohler, G. Rizzoni, M. Bargende, and S. Haas, "Mixed-mode diesel HCCI with external mixture formation: preliminary results", *FKFS Germany*, Vol. 14, No. 1, pp. 1-34, (2003).
- [7] R. Jyothu Naik and Thirupathi Reddy Kota, "Influences of pilot injection, main injection and EGR on performance combustion and emissions in an HCCI-DI combustion engine using with Diesel and WPPO bio-diesel blends", *Int. J. Ambient Energy*, Vol. 43, No. 1, pp. 2376-2391, (2020).
- [8] D. Damodharan, A. P. Sathiyagnanam, D. Rana, B. R. Kumar and S. Saravanan, "Combined influence of injection timing and EGR on combustion, performance and emissions of DI diesel engine fueled with neat waste plastic oil", *Energy Convers Manag.*, Vol. 161, No. 1, pp. 294-305, (2018).
- [9] S. Murugan, M. C. Ramaswamy, and G. Nagarajan, "Assessment of pyrolysis oil as an energy source for diesel engines", *Fuel. Process Technol.*, Vol. 90, No. 1, pp. 67-74, (2009).
- [10] D. Damodharan, K. Gopal, A. P. Sathiyagnanam, B. Rajesh Kumar, M. V. Depoures and N. Mukilarasan, "Performance and emission study of a single cylinder diesel engine fuelled with n-octanol/WPO with some modifications", *Int. J. Ambient Energy*, Vol. 42, No. 7, pp. 779-788, (2021).
- [11] O. D. Samuel, M. O. Okwu, S. T. Amosun, T. N. Verma and S. A. Afolalu, "Production of fatty acid ethyl esters from rubber seed oil in hydrodynamic cavitation reactor study of reaction parameters and some fuel properties", *Ind. Crops Prod*, Vol. 141, No. 1, pp. 141-148, (2019).
- [12] T. S. Singh, and T. N. Verma, "An analysis on the effect of temperature on the morphology of egg shell CaO catalyst: Caytalyst production for biodiesel

- preparation", *Int. J. Science Techno*, Vol. 27, No. 6, pp. 2915-2923, (2019).
- [13] S. Srihari, S. Thirumalini, and K. Prashanth, "An experimental study on the performance and emission characteristics of PCCI-DI engine fuelled with diethyl ether-biodiesel-dieselblends", *Renew. Energy*, Vol. 107, No. 1, pp. 440-447, (2017).
- [14] S. S. Kalsi, and K. A. Subramanian, "Effect of simulated biogas on performance, combustion and emissions characteristics of a bio-diesel fueled diesel engine", *Renew. Energy*, Vol. 106, Vol. 2, pp. 78-90, (2017).
- [15] S. Prabu, M. A. Senthur, A. Rahul Roy, S. Francis, and M. K. Sreelekh, "Performance, combustion and emission characteristics of diesel engine fuelled with waste cooking oil bio-diesel/diesel blends with additives", *Energy*, Vol. 122, No. 1, pp. 638-648, (2017).
- [16] Heywood and B. John, "*Internal Combustion Engine Fundamentals*", 2nded., McGraw Hill Press, New York, pp. 58-65, (1988).
- [17] J. A. Gatowski, E. N. Balles, Kchun. M, Nelson. F. E, Ekchian. J. A, and Heywood, "Heat release analysis of engine pressure data", *Sae. Trans*, Vol. 93, No. 5, pp. 961-977, (1984).
- [18] M. A. Ceviz, and I. Kaymaz, "Temperature and air-fuel ratio dependent specific heat ratio functions for lean burned and unburned mixture", *Energy. Convers Manag.*, Vol. 46, No. 15-16, pp. 2387-2404, (2005).
- [19] M. Christensen, "*HCCI Combustion Engine Operation and Emission Characteristics*", PhD Thesis, Dept. Heat & Power Eng., Div. of Comb. Engines, Lund University, Sweden, (2002).
- [20] A. K. Agarwal, A. P. Singh, J. Lukose, and T. Gupta, "Characterization of exhaust particulates from diesel fueled homogenous charge compression ignition combustion engine", *J. Aerosol Sci.*, Vol. 58, pp. 71-85, (2013).
- [21] D. Ganesh, and G. Nagarajan, "Homogeneous charge compression ignition (HCCI) combustion of diesel fuel with external mixture formation", *Energy*, Vol. 35, No. 1, pp. 148-157, (2010).
- [22] B. Harisankar, and S. Murugan, "Experimental investigation on the effect of charge temperature on ethanol fueled HCCI combustion engine", *J. Mech. Sci Technol*, Vol. 30, No. 10, pp. 4791-4799, (2016).

Copyrights ©2024 The author(s). This is an open access article distributed under the terms of the Creative Commons Attribution (CC BY 4.0), which permits unrestricted use, distribution, and reproduction in any medium, as long as the original authors and source are cited. No permission is required from the authors or the publishers.



How to cite this paper:

R. Jyothu Naik, K. Thirupathi Reddy and S. Vishal Narayanrao, "Effect of exhaust gas recirculation and constant pre-heated air temperature on the homogeneous charge compression ignition combustion engine with diesel and WPO 20 blend," *J. Comput. Appl. Res. Mech. Eng.*, Vol. 13, No. 2, pp. 157-167, (2024).

DOI: 10.22061/JCARME.2023.8413.2135

URL: https://jcarme.sru.ac.ir/?_action=showPDF&article=2018

